Experimentally Inferred Fusion-Yield Dependencies of OMEGA Inertial Confinement Fusion Implosions

A. Lees,[1,2] R. Betti,[1,2,3] J. P. Knauer,[1] V. Gopalaswamy,[1,2] D. Patel,[1,2] K. M. Woo,[1] K. S. Anderson,[1] E. M. Campbell,[1] D. Cao,[1] J. Carroll-Nellenback,[1] R. Epstein,[1] C. J. Forrest,[1] V. N. Goncharov,[1] D. R. Harding,[1] S. X. Hu,[1] I. V. Igumenshchev,[1] R. T. Janezic,[1] O. M. Mannion,[1,3] P. B. Radha,[1] S. P. Regan,[1] A. Shvydky,[1] R. C. Shah,[1] W. T. Shmayda,[1] C. Stoeckl,[1] W. Theobald,[1] and C. A. Thomas[1]

[1]Laboratory for Laser Energetics, University of Rochester
[2]Department of Mechanical Engineering, University of Rochester
[3]Department of Physics and Astronomy, University of Rochester

Inertial confinement fusion[1] implosions are complex nonlinear processes that are highly sensitive to many input parameters. The lack of an accurate simulation capability, the low shot rate of laser implosion facilities, and the effects of shot-to-shot variations make it difficult to extract single parameter dependencies, thereby preventing guided improvements in implosion performance. In this summary, the different dependencies of the fusion yield are extracted from the OMEGA[2] experimental database of 177 implosions. The importance of these results is twofold: First, they identify the degradation mechanisms; second, they enable predictions of how the yield improves if each degradation is mitigated. When applied to OMEGA implosions the results indicate that the highest yield achievable on OMEGA should exceed 2×10^{14} neutrons with only minor adjustment to the laser pointing and by reducing the fill age. Yields close to 3×10^{14} are predicted if the degradation from $R_\mathrm{b}/R_\mathrm{t}$ is mitigated.

Generalizing the conclusions of Ref. 3 to include the effects of variable systematic nonuniformity seeds and experimental input parameters that are not included in 1-D simulations, a physics-based statistical mapping model [see Eq. (1)] is derived for the measured fusion yield Y^{exp}. The yield is assumed to be dominated by the implosion velocity, which is typically well simulated by the 1-D code *LILAC*,[4] as indicated by shell trajectory measurements;[5] therefore, the yield is expected to depend on the simulated 1-D yield $Y_{\text{1-D}}^{\mathrm{sim}}$. The statistical model is written in terms of the yield-over-clean (YOC), leading to the following intuitive formulation of the fusion yield:

$$
\begin{aligned}
Y^{\mathrm{exp}} &= \mathrm{YOC}^{\mathrm{exp}} Y_{\text{1-D}}^{\mathrm{sim}} \\
\mathrm{YOC}^{\mathrm{exp}} &\approx \mathrm{YOC_h YOC_f YOC_b YOC_{\ell=1} YOC_{res}},
\end{aligned}
\tag{1}
$$

where the degradation due to hydrodynamic instabilities from systematic nonuniformities is denoted as $\mathrm{YOC_h}$; $\mathrm{YOC_f}$ is the degradation due to DT fill age, tritium damage, and ^{3}He accumulation; $\mathrm{YOC_b}$ is the degradation from finite laser beam size; and $\mathrm{YOC}_{\ell=1}$ is the degradation from the $\ell = 1$ mode. $\mathrm{YOC_{res}}$ denotes a weak (≤15% over the entire database) residual size scaling not captured by 1-D hydrocodes[6,7] and is approximately constant for high-performance OMEGA implosions. Each YOC term is analyzed and extracted by mapping onto the experimental database.

The yield degradation from $\ell = 1$ can be approximated as a power law of the temperature ratio between the maximum and minimum apparent ion temperature $R_T = T_1^{\max}/T_1^{\min}$ (Ref. 8). Since the T_i measurement error is about 10%, only implosions with R_T greater than a minimum threshold $R_T^{\min} \approx 1.1$ are expected to exhibit detectable degradation. Therefore, the degradation from the $\ell = 1$ mode is approximated as

$$\mathrm{YOC}_{\ell=1} \sim \hat{R}_T^{\mu}, \hat{R}_T \equiv \max\left[1, \frac{R_T}{R_T^{\min}}\right]. \tag{2}$$

Here the values of μ and $R_T^{\min}$ are obtained through the global mapping onto the data.

$\mathrm{YOC_f}$ depends on the time between the DT fill and the shot time (fill age) as well as the tritium and deuterium concentrations (θ_T and θ_D, respectively). Instead of the fill age, one can use the 1-D–simulated yield degradation $\xi\mathrm{He} = Y_{\text{1-D,He}}^{\text{sim}}/Y_{\text{1-D}}^{\text{sim}}$, where $Y_{\text{1-D,He}}^{\text{sim}}$ includes the ^{3}He produced over the course of the fill age, all of which is assumed to be accumulated in the vapor region. Power-law dependencies are assumed, leading to

$$\mathrm{YOC_f} \sim \theta_\mathrm{T}^{\delta}\theta_\mathrm{D}^{\nu}\xi_\mathrm{He}^{\phi}. \tag{3}$$

The degradation from finite laser spot size $\mathrm{YOC_b}$ can be approximated through a power of laser beam to target radius $R_\mathrm{b}/R_\mathrm{t}$:

$$\mathrm{YOC_b} \sim \left(R_\mathrm{b}/R_\mathrm{t}\right)^{\gamma} \tag{4}$$

with $\gamma \approx 2.4$ in 3-D simulations.[9] Here, as for all the other degradations, the exponent γ is determined by the mapping to the data.

A functional relation of simulated 1-D parameters that best maps the degradation from hydrodynamic instabilities, $\mathrm{YOC_h}$ is constructed by combining in-flight aspect ratio (IFAR) and the shell adiabat $\alpha_\mathrm{F} = P_\mathrm{a}/P_\mathrm{F}$ (ratio of the ablation pressure to the Fermi degenerate pressure), into a single parameter $I_\alpha \equiv \left(\alpha_\mathrm{F}/3\right)^{1.1}/(\mathrm{IFAR}/20)$ as indicated in Refs. 10 and 11. The convergence ratio (CR) is added to better account for the degradation from low- and mid-mode asymmetries. To account for inaccuracies in modeling shock transit, the shell thickness is included through the dimensionless parameter $\hat{D} \equiv R_\mathrm{out}/R_\mathrm{in}$ representing the ratio between the outer and inner shell radii. Therefore $\mathrm{YOC_h}$ is approximated as $\mathrm{YOC_h} \sim I_\alpha^{\eta}\mathrm{CR}^{\hat{\omega}}D^{\varepsilon}$. At sufficiently large adiabats and low IFAR's, implosions become stable to short-wavelength modes and the benefits of higher adiabat and low IFAR are expected to decrease.[10] Therefore, a piecewise value of η is used above and below a critical value (I_c) of I_α. The final form of the hydrodynamic degradation is then written as

$$\mathrm{YOC_h} \sim \hat{I}_\alpha^{\eta} C_R^{\omega} D^{\varepsilon}, \tag{5}$$

where $\hat{I}_\alpha = I_\alpha/I_\mathrm{c}$ and $\eta = \eta_< \Theta\left(1 - \hat{I}_\alpha\right) + \eta_> \Theta\left(\hat{I}_\alpha - 1\right)$ with $\Theta(x)$ representing the Heaviside step function.

The power indices in Eqs. (2)–(5) are determined by χ^2 minimization over the entire OMEGA implosion database and the two threshold parameters $R_T^{\min}$, I_c were chosen to minimize the cross-validation error. The results are summarized in Table I including the 95% confidence level for each exponent. Each dependence can be visualized by isolating the corresponding YOC and comparing with the power-law approximation:

$$\mathrm{YOC}_j^{\exp} \equiv \frac{\mathrm{YOC}^{\exp}}{\Pi_{i \neq j}\mathrm{YOC}_i} \to \mathrm{YOC}_j. \tag{6}$$

The plots in Fig. 1 show the comparison in Eq. (6) for the dependencies in Eq. (1).

General conclusions can be readily extracted from this analysis. First, the degradation from the $\ell = 1$ is as predicted by the 3-D simulations with a power index $\mu \approx -1.44$ and a threshold factor $R_T^{\min} = 1.14$ from the T_i measurement error. Such a good agreement with the simulations confirms the accuracy of the mapping technique to extract the correct trends from the data. Reasonable agreement with 1-D–simulated degradation due to ^{3}He accumulation is indicated by $\varphi \approx 1.39$ close to unity. Furthermore, the degradation in two extremely long fill age targets (45 and 90 days) is well predicted as shown by the two points farthest to the left on Fig. 1(b), adding confidence that the model is correctly accounting for the effect of ^{3}He accumulation. As a result of this

Table I: Power indices and confidence intervals for all the degradation terms as a result of fitting the model in Eq. (1) to the OMEGA database.

Parameter	Power index	95% confidence interval
$\hat{R}_T^{\mu}$	$\mu = -1.44$ $R_{\mathrm{T}}^{\mathrm{min}} = 1.14$	$\mu = -1.61$ to -1.28
ξ_{He}^{ϕ}	$\phi = 1.39$	$\phi = 1.25$ to 1.54
$\theta_{\mathrm{T}}^{\delta}$	$\delta = 1.97$	$\delta = 1.00$ to 2.90
$\theta_{\mathrm{D}}^{\nu}$	$\nu = 1.16$	$\nu = 0.54$ to 1.79
$(R_{\mathrm{b}}/R_{\mathrm{t}})^{\gamma}$	$\gamma = 2.97$	$\gamma = 2.72$ to 3.24
$\hat{I}_{\alpha}^{\eta}$	$\eta_< = 1.06$ $\eta_> = 0.45$ $I_{\mathrm{c}} = 0.8$	$\eta_< = 0.91$ to 1.21 $\eta_> = 0.40$ to 0.49
C_R^{ω}	$\omega = -0.97$	$\omega = -1.05$ to -0.89
$\hat{D}^{\varepsilon}$	$\varepsilon = -3.35$	$\varepsilon = -4.11$ to -2.58

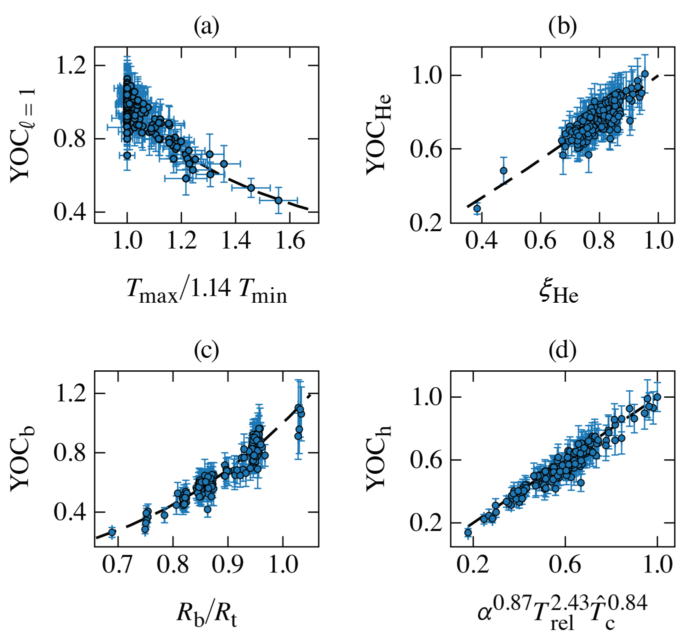

Figure 1
The individual degradations due to (a) $\ell = 1$ mode, (b) ^{3}He accumulation in the vapor, (c) finite beam size, and (d) hydrodynamic instabilities extracted from the OMEGA database according to Eq. (6). The dashed lines indicate the power laws from the model; the power indices are given in Table I.

analysis, OMEGA shot 96806 was designed with the shortest-ever fill age of 3 days, achieving the highest performance on OMEGA at the time with a neutron yield of 1.53×10^{14} and an areal density of 157±15 mg/cm^2 at a laser energy of 27.3 kJ.

Shot 96806 was subsequently repeated with a fill age of 8 days (shot 96808) resulting in a 14% reduction in fusion yield, as predicted by the statistical model (13%). Another conclusion can be drawn about the isotopic composition of the DT ice layer since maximizing the term $\theta_{\mathrm{T}}^{1.97}\ (1-\theta_{\mathrm{T}})^{1.16}$ gives the optimal tritium concentration at $\theta_{\mathrm{T}} \approx 0.6$. The mapping to data reveals a strong $R_{\mathrm{b}}/R_{\mathrm{t}}$ correlation with a power index of $\gamma = 2.97$, which is stronger than indicated by 3-D simulations of the beam mode in Ref. 9. Furthermore, the highest-performing implosions with $R_{\mathrm{b}}/R_{\mathrm{t}} \approx 0.87$ show a significant (35%) degradation from this mechanism, whereas post-shot 3-D simulations show negligible degradation due to the beam mode. This indicates that new physics is at play, which is an active area of research, and it can include new sources of nonuniformities from the laser beam geometry as well as 1-D physics model deficiencies most likely related to the reduction of cross-beam energy transfer, when $R_b < R_t$. Lastly, the mapping model indicates strong degradation due to hydrodynamic effects (YOC_h) at low adiabat, high convergence, and high IFAR [Fig. 1(d)]. The results indicate that the highest yields can be achieved only at high adiabat and low IFAR with the maximum yield occurring at adiabats >4.5.

This material is based upon work supported by the Department of Energy National Nuclear Security Administration under Award Number DE-NA0003856, the University of Rochester, and the New York State Energy Research and Development Authority.

1. J. Nuckolls *et al*., Nature **239**, 139 (1972).
2. T. R. Boehly *et al*., Opt. Commun. **133**, 495 (1997).
3. V. Gopalaswamy *et al*., Nature **565**, 581 (2019).
4. J. Delettrez *et al*., Phys. Rev. A **36**, 3926 (1987).
5. D. T. Michel *et al*., Phys. Rev. Lett. **114**, 155002 (2015).
6. W. Theobald *et al*., “OMEGA Subscale Cryogenic Implosions in Symmetric and Polar-Direct-Drive Beam Geometry,” presented at the 62nd Annual Meeting of the American Physical Society Division of Plasmas Physics, Memphis, TN, 9–13 November 2020.
7. C. A. Thomas *et al*., “Quantifying the Effects of Scale and Illumination Geometry in Laser Direct Drive,” presented at the 62nd Annual American Physical Society Division of Plasma Physics, Memphis, TN, 9–13 November 2020.
8. K. M. Woo *et al*., Phys. Plasmas **27**, 062702 (2020).
9. V. Gopalaswamy *et al*., “Using Statistics to Predict, Design, and Understand Fusion Experiments,” submitted to Physics of Plasmas.
10. V. N. Goncharov *et al*., Phys. Plasmas **21**, 056315 (2014).
11. H. Zhang *et al*., Phys. Plasmas **27**, 122701 (2020).